*American Mineralogist, Volume 90, pages 1556–1562, 2005*

# Does the bazhenovite structure really contain a thiosulfate group? A structural and spectroscopic study of a sample from the type locality

**Luca Bindi,[1,2,*] Paola Bonazzi,[1] Luigi Dei,[3,4] and Angela Zoppi[3]**

[1]Dipartimento di Scienze della Terra, Università degli Studi di Firenze, Via La Pira, 4-I-50121 Firenze, Italy
[2]Museo di Storia Naturale, Sezione di Mineralogia, Università degli Studi di Firenze, Via La Pira, 4 - I-50121 Firenze, Italy
[3]Dipartimento di Chimica, Università degli Studi di Firenze, Via della Lastruccia, 3-I-50019 Sesto Fiorentino, Firenze, Italy
[4]Consorzio Interuniversitario per lo sviluppo dei Sistemi a grande Interfase, Via della Lastruccia, 3-I-50019 Sesto Fiorentino, Firenze, Italy

## Abstract

Bazhenovite was originally reported as a rare, thiosulfate-containing mineral, with the chemical formula $CaS_5 \cdot CaS_2O_3 \cdot 6Ca(OH)_2 \cdot 20H_2O$. The structure was predicted to be layered, but no structural details were given. A crystal of "bazhenovite" from the pyritized siderite fragments occurring in the melt products of burning dumps at the type locality in the Chelyabinsk coal basin, South Urals, Russia has been examined by single-crystal X-ray diffraction and vibrational spectroscopy (FTIR and Raman). The structure was solved in space group $P2_1/c$ and refined assuming twinning on {100} to a final $R_{obs}$ = 5.03% (731 reflections) and $R_{all}$ = 6.98% (966). Although the unit-cell dimensions of the examined crystal [$a$ = 8.391(2), $b$ = 17.346(6), and $c$ = 8.221(4) Å, β = 119.33(5)°, $V$ = 1043.2(8) Å$^3$ ] match those of the original bazhenovite description [$a$ = 8.45(1), $b$ = 17.47(1), and $c$ = 8.24(1) Å, β = 119.5°, $V$ = 1059 Å$^3$ ], the thiosulfate group was not detected by either structural analysis or spectroscopic investigations. The structure is an alternating sequence of two kinds of layers, labeled A and B respectively, stacked along [010]. The A layer is the ordered part of the structure and consists of a linkage of $Ca(OH)_2(H_2O)_6$ antiprisms and $Ca(OH)_4(H_2O)_2$ octahedra. Taking into account both structural and spectroscopic results, the B layer is inferred to consist of a disordered assemblage of $S_3^{2-}$, and to a lesser extent, $S_4^{2-}$ groups, with the possible presence of additional $H_2O$ and $H_2S$. The possibility that bazhenovite and the mineral here examined could represent two distinct phases differing slightly from each other with respect to the thiosulfate content is discussed.

## Introduction

Bazhenovite is a rare mineral first described by Chesnokov et al. (1987) associated with native iron, native sulfur, oldhamite, troilite, pyrrhotite, fluorite, and periclase in altered pyritized siderite fragments in the melt products of burning dumps in the Chelyabinsk coal basin (South Urals, Russia). On the basis of wet-chemical analysis, TGA results, and infrared spectroscopic data, Chesnokov et al. (1987) assigned the chemical formula $CaS_5 \cdot CaS_2O_3 \cdot 6Ca(OH)_2 \cdot 20H_2O$ and classified the mineral as a hybrid hydrate calcium hydroxide-polysulfide-thiosulfate. Both the chemical composition and the X-ray powder diffraction pattern are similar to that of the orthorhombic compound ($a$ = 14.67, $b$ = 17.65, $c$ = 8.254 Å; space group not reported) synthesized by Lutz et al. (1969). According to Chesnokov et al. (1987), bazhenovite is monoclinic, space group $P2_1/c$, $a$ = 8.45(1), $b$ = 17.47(1), and $c$ = 8.24(1) Å, β = 119.5°, $V$ = 1059 Å$^3$. The structure was thought to be layered, but no structural details were given.

More recently, Witzke and Göske (2002) described another occurrence of bazhenovite from the Ronneburg uranium mining area (Thuringia, Germany). These authors pointed out the role of gases, namely $H_2S$ and $SO_2$, in the alteration of oldhamite (CaS) leading to the formation of several secondary minerals associated with bazhenovite, including hannebachite [$Ca(SO_3) \cdot 0.5H_2O$], ettringite [$Ca_6Al_2(SO_4)_3(OH)_{12} \cdot 26H_2O$], portlandite [$Ca(OH)_2$], and gypsum. The study carried out by Witzke and Göske (2002) deals with the equilibrium/disequilibrium of the mineral association and does not report any X-ray characterization of the studied minerals. In this paper, we report a structural model for a bazhenovite-like crystal from the type locality. Because of the long period of time elapsed since its discovery, a question could arise as to whether or not the mineral studied here is still unaltered bazhenovite or has lost some components with respect to the original sample.

## Experimental methods

Numerous crystals were mounted on an Enraf-Nonius CAD4 single-crystal diffractometer and examined with graphite-monochromatized Mo$K\alpha$ X-radiation. Most were found to be composed of minute aggregates. Diffraction peaks were broad and rather weak. A crystal (80 × 80 × 100 μm, approximately) of fair diffraction quality was selected for the structural study.

Unit-cell dimensions were determined by least-squares refinement of the setting angles of 25 high-θ reflections ($10 < \theta_{MoK\alpha} < 12°$) giving $a$ = 8.221(4), $b$ = 14.631(3), and $c$ = 17.346(6) Å, $V$ = 2086.4(13) Å$^3$. Intensity data were collected ($\bar{8} < h < 8$, $\bar{16} < k < 16$, $0 < l < 7$) in the range $2 < \theta_{MoK\alpha} < 20°$, ω-scan mode, with a scan width of 3.2°, and a scan speed of 1.65°/min. Intensities were treated for Lorentz-polarization effects and subsequently corrected for absorption following the semi-empirical method of North et al. (1968) using the 860 and $\bar{8}\bar{6}0$ reflections ($\chi = \pm 89.81°$).

FTIR spectra were collected using a Bio-Rad FTS-40 spectrometer in the range 400–4000 cm$^{-1}$ with the KBr pellet technique at 4 cm$^{-1}$ resolution and 32 scans.

Raman spectra were collected from single crystals by the micro-Raman tech-

* E-mail: lbindi@geo.unifi.it

nique using an argon laser (514.5 nm emission). Measurement conditions were as follows: power on sample 3.5 mW, magnification objective 50×, spatial resolution 1 μm, spectral resolution 7 $cm^{-1}$, collecting time 100–600 s.

## Structure solution and refinement

The analysis of systematic absences (*hkl*: $h + k = 2n$; 0*kl*: $k = 2n$; *h*0*l*: $h, l = 2n$; *hk*0: $h, k = 2n$; *h*00: $h = 2n$; 0*k*0: $k = 2n$; 00*l*: $l = 2n$) suggested *Cmca* or *C*2*ca* (*Aba*2 as standard) as possible space group choices. Statistical tests on the distribution of |E| values ($|E^2-1| = 0.966$) indicated a centrosymmetric structure. Equivalent structure factors were merged in the Laue class *mmm* ($R_{symm} = 3.33\%$). The first attempt to solve the structure by direct methods using SHELXS-97 (Sheldrick 1997a) was performed in space group *Cmca*. The positions of the Ca and O atoms were located on an $F_o$-Fourier map (layers at $z = ¼, ¾$). The Δ*F*-Fourier synthesis calculated with structure factors phased by the contribution of these atoms showed several residual peaks located at $z = 0, ½$, tentatively assigned as partially occupied S positions. The full-matrix least-squares program SHELXL-97 (Sheldrick 1997b) was used for the refinement of the structure done on $F^2$. Scattering curves for neutral Ca, S, and O were taken from *International Tables for X-ray Crystallography*, volume IV (Ibers and Hamilton 1974). Refinement of the anisotropic atomic displacement parameters for all the atoms but S led to an *R*1 index of 10.77% for 426 observed reflections [$F_o > 4\sigma(F_o)$] and $R = 12.32\%$ for all 532 independent reflections. However, a careful analysis of the intensity data showed 24 systematic absence violations [$F_o/\sigma(F_o) > 7$] for *h*0*l* reflections with $l = 2n + 1$. Therefore, it was hypothesized that the true symmetry was monoclinic with apparent orthorhombic pseudosymmetry due to twinning. Among the maximal non-isomorphic monoclinic subgroups of *Cmca* (*C*2/*m*11, *C*12/*c*1, $C112_1/a$), only $C112_1/a$ ($P2_1/c$ as standard) is totally consistent with the observed systematic absences, in keeping with the best internal consistency ($R_{symm} = 1.99\%$) found by setting the monoclinic unique axis along the orthorhombic **c** axis. The unit-cell parameters and the reflection indices were then transformed according to the matrix [–½ ½ 0 / 0 0 1 / 1 0 0] and the following values were obtained: $a = 8.391(2)$, $b = 17.346(6)$, and $c = 8.221(4)$ Å, $\beta = 119.33(5)°$, $V = 1043.2(8)$ $Å^3$.

Assuming twinning on {100}, the structure was solved in $P2_1/c$ and refined following the method of Pratt et al. (1971) for merohedric twinned structures. The refined value of the fraction of the first twin component was 0.49, in keeping with the relatively low value (3.33%) of $R_{symm}$ in the *mmm* Laue group. The Δ*F*-Fourier synthesis calculated with structure factors phased by the contribution of Ca and O atoms (layers at $y = ¼, ¾$ in the monoclinic orientation) still showed several residual peaks located at $y = 0, ½$. These were tentatively assigned as partially occupied S positions and their isotropic displacement parameters were initially kept fixed at 0.05 $Å^2$ (the SHELXL default value). Successive least squares cycles were run by alternately fixing the site-occupancy factors and the isotropic displacement parameters for each of the S atoms. Final occupancy factors for the S1 to S6 positions were 0.44, 0.44, 0.34, 0.51, 0.23, and 0.23, respectively. The S-site occupancies were then fixed and an anisotropic model was refined for the entire structure. Convergence was achieved quickly to $R = 8.88\%$ for 731 observed reflections [$F_o > 4\sigma(F_o)$] and 10.77% for all 966 independent reflections. Nevertheless, inspection of the Δ*F*-Fourier map showed two significant residual peaks of about 2.1 and 1.8 $e^-/Å^3$ about 1.24 Å from each other. The introduction of these additional peaks (Ow1 and Ow2), tentatively assigned as partially occupied O positions [with a constraint fixing (s.o.f. Ow1 + s.o.f. Ow2) = 1.00] significantly improved the *R* indices [$R_{obs} = 6.05\%$ (731), $R_{all} = 7.96\%$ (966)]. Two more peaks at 0.94 and 0.87 Å from Ow1, respectively, were also located and assigned as hydrogen atoms (labeled Hw1 and Hw2, respectively). Finally, eight other residual peaks suitable as hydrogen atoms were located. An attempt to refine the hydrogen positions, however, was unsuccessful. Therefore, both fractional coordinates and isotropic displacement parameters for the hydrogen atoms were fixed. The final *R* indices were $R_{obs} = 5.03\%$ (731) and $R_{all} = 6.98\%$ (966). Inspection of the Δ*F*-Fourier map revealed that maximum positive and negative peaks were 0.33 and 0.35 $e^-/Å^3$, respectively. Final fractional atomic coordinates, site occupancies and anisotropic displacement parameters are listed in Table 1. Table 2[1] lists the observed and calculated structure factors.

## FTIR and Raman characterization

FTIR spectra did not show the features typical of the $S_2O_3^{2-}$ species; in particular the strong absorption due to $\nu_{SO}$ asymmetric at 1130 $cm^{-1}$ (Lutz et al. 1969; Ross 1972; Braithwaite et al. 1993) was not observed. Moreover, other sharp absorption maxima characteristic of the thiosulfate anion at 1019, 687, 554, and 527 $cm^{-1}$ (Ross 1972; Braithwaite et al. 1993) were not detected in our sample. However, a well-resolved sharp peak at 502 $cm^{-1}$ due to the stretching $\nu_{SS}$ of the $S_3^{2-}$ polyion (Lutz et al. 1969) was present. These data, therefore, inferred the presence of sulfur in the form of $S_n^{2-}$ polyions alone, which accounts for the typical yellow-orange color of bazhenovite. A sharp peak at 3646 $cm^{-1}$ indicated the presence of $OH^-$ anions linked to $Ca^{2+}$ cations, in agreement with the OH stretching at 3642 $cm^{-1}$ observed in the spectrum of portlandite (Ryskin 1974). Finally, the FTIR spectrum evidenced the broad absorption attributed to crystallization water around 3420 $cm^{-1}$.

Micro-Raman spectra originated from single crystals confirmed these findings. In particular, the spectrum collected with the 514.5 nm excitation line (Fig. 1) showed the peak at 507 $cm^{-1}$ that is typical of the $S_3^{2-}$ group (Lutz et al. 1969). The other strong peak at 466 $cm^{-1}$ (Fig. 1) cannot be ascribed to the $S_2O_3^{2-}$ ion since the Raman spectrum of this species presents one strong peak, possibly with a doublet shape, in the region between 430 and 470 $cm^{-1}$, and many medium intensity peaks in the ranges 985–1015, 66–680, and 320–360 $cm^{-1}$ (Degen and Newman 1993). The Raman spectrum did not give any evidence of these spectral characteristics, indicating unambiguously that

[1] Deposit item AM-05-022, Table 2. Deposit items are available two ways. For a paper copy contact the Business Office of the Mineralogical Society of America (see inside front cover of recent issue) for price information. For an electronic copy visit the MSA web site at http://www.minsocam.org, go to the American Mineralogist Contents, find the table of contents for the specific volume/issue wanted, and then click on the deposit link there.

**TABLE 1.** Fractional coordinates and anisotropic displacement parameters $U_{ij}$ (Å$^2$) for the crystal examined

| | s.o.f. | *x* | *y* | *z* | $U_{11}$ | $U_{22}$ | $U_{33}$ | $U_{12}$ | $U_{13}$ | $U_{23}$ | $U_{eq}$ |
|---|---|---|---|---|---|---|---|---|---|---|---|
| Ca1 | 1.0 | 0.2548(2) | 0.2476(2) | 0.3706(3) | 0.020(1) | 0.039(1) | 0.015(3) | –0.010(2) | 0.005(2) | –0.005(1) | 0.0261(6) |
| Ca2 | 1.0 | 0.7542(3) | 0.2475(3) | 0.6201(3) | 0.020(1) | 0.046(1) | 0.012(3) | 0.006(2) | 0.003(3) | 0.003(1) | 0.0279(6) |
| O1 | 1.0 | 0.1303(7) | 0.3186(4) | 0.0641(14) | 0.038(4) | 0.036(4) | 0.030(6) | –0.001(3) | 0.016(5) | 0.002(5) | 0.035(2) |
| O2 | 1.0 | 0.3739(7) | 0.3207(4) | 0.6730(13) | 0.014(3) | 0.053(4) | 0.014(5) | –0.004(3) | 0.008(4) | –0.002(4) | 0.027(2) |
| O3 | 1.0 | 0.7512(8) | 0.3153(4) | 0.8665(10) | 0.023(3) | 0.045(4) | 0.031(6) | –0.001(3) | 0.014(6) | 0.001(4) | 0.033(2) |
| O4 | 1.0 | 0.5105(8) | 0.3231(4) | 0.3983(11) | 0.013(4) | 0.044(4) | 0.029(5) | –0.012(4) | 0.003(4) | –0.005(4) | 0.032(2) |
| O5 | 1.0 | 0.0007(9) | 0.1745(4) | 0.1438(10) | 0.030(6) | 0.044(5) | 0.023(4) | –0.003(3) | 0.025(4) | –0.004(4) | 0.027(2) |
| O6 | 1.0 | 0.5063(8) | 0.1722(3) | 0.5943(9) | 0.038(4) | 0.038(3) | 0.008(4) | –0.006(3) | 0.013(3) | –0.007(3) | 0.027(2) |
| O7 | 1.0 | –0.0036(9) | 0.3249(4) | 0.3393(10) | 0.020(5) | 0.043(5) | 0.041(5) | 0.001(3) | 0.012(4) | –0.001(4) | 0.036(2) |
| Ow1 | 0.60(2) | 0.350(2) | 0.496(1) | 0.816(3) | 0.058(9) | 0.060(10) | 0.080(13) | –0.007(8) | 0.024(11) | –0.002(9) | 0.070(5) |
| Ow2 | 0.40 | 0.312(3) | 0.473(1) | 0.658(6) | 0.100(19) | 0.016(15) | 0.179(42) | 0.055(14) | 0.090(30) | 0.049(21) | 0.089(12) |
| S1 | 0.44(1) | 0.811(2) | 0.504(1) | 0.897(2) | 0.061(6) | 0.055(6) | 0.030(9) | –0.006(4) | 0.019(8) | –0.001(7) | 0.050(3) |
| S2 | 0.44(2) | 0.761(2) | 0.502(1) | 0.786(2) | 0.095(11) | 0.028(4) | 0.034(8) | 0.005(6) | 0.040(9) | –0.003(7) | 0.049(3) |
| S3 | 0.34(2) | 0.904(3) | 0.500(1) | 0.672(3) | 0.136(15) | 0.089(10) | 0.086(16) | –0.032(11) | 0.084(15) | –0.028(16) | 0.091(5) |
| S4 | 0.51(2) | –0.006(2) | 0.498(1) | 0.199(2) | 0.169(12) | 0.053(5) | 0.056(9) | –0.021(7) | 0.055(10) | –0.012(7) | 0.092(4) |
| S5 | 0.23(2) | 0.580(4) | 0.499(1) | 0.653(3) | 0.090(18) | 0.106(16) | 0.016(15) | –0.005(13) | 0.009(17) | –0.021(12) | 0.078(6) |
| S6 | 0.23(2) | 0.438(3) | 0.494(1) | 0.520(3) | 0.104(16) | 0.038(9) | 0.037(13) | 0.001(10) | 0.056(12) | 0.005(11) | 0.050(5) |
| H1a | 1.0 | 0.004 | 0.312 | 0.004 | | | | | | | |
| H1b | 1.0 | 0.173 | 0.368 | 0.108 | | | | | | | |
| H2a | 1.0 | 0.500 | 0.320 | 0.745 | | | | | | | |
| H3b | 1.0 | 0.770 | 0.367 | 0.853 | | | | | | | |
| H4b | 1.0 | 0.499 | 0.383 | 0.407 | | | | | | | |
| H46a | 1.0 | 0.508 | 0.325 | 0.247 | | | | | | | |
| H5b | 1.0 | –0.040 | 0.377 | 0.649 | | | | | | | |
| H57a | 1.0 | –0.002 | 0.325 | 0.491 | | | | | | | |
| Hw1 | 0.60 | 0.288 | 0.497 | 0.875 | | | | | | | |
| Hw2 | 0.60 | 0.351 | 0.531 | 0.729 | | | | | | | |

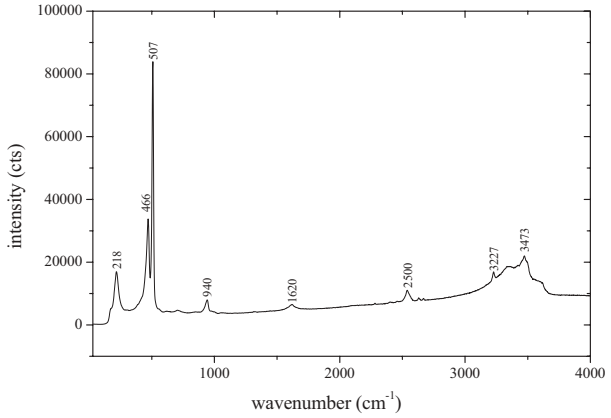


**FIGURE 1.** Raman spectrum collected using an argon laser with an emission of 514.5 nm.

there is no thiosulfate group in the mineral structure. Moreover, the peak at 466 cm$^{-1}$ and the weaker peak at 218 cm$^{-1}$ can be attributed to polyions of the type $S_4^{2-}$ or $S_5^{2-}$, excluding the presence of $S_n^{2-}$ with $n \geq 6$ for which the Raman spectra show peaks at wavenumbers below 400 cm$^{-1}$ (Janz et al. 1976a, 1976b, 1976c; Chivers and Lau 1982).

The Raman spectrum also indicated the presence of crystallization water ($\delta_{H_2O}$ at 1620 cm$^{-1}$ and peaks due to the $\nu_{OH}$ in the region 3000–3600 cm$^{-1}$). Finally, the series of signals at about 2500 cm$^{-1}$ could be attributed to the presence of $H_2S$ species in their condensed form (Herzberg 1945).

## DESCRIPTION OF THE STRUCTURE

The structure of the crystal examined consists of a sequence of two different layers (A and B) parallel to (010) (Fig. 2).

The A-layer (*y* = ¼, ¾) can be described as a linkage of two independent chains sharing O-O edges, both running along [001]: the first consists of Ca1 square antiprisms linked together by sharing opposite edges, the second is formed by corner-sharing Ca2 octahedra (Fig. 3). The Ca1-O bond distances are in the range 2.395–2.58 Å (Table 3), with a mean value of 2.482 Å which compares favorably with that observed in other structures wherein Ca ions are coordinated by eight OH and/or $H_2O$ oxygen atoms (e.g., 2.50 and 2.51 Å in ettringite, Moore and Taylor 1970; 2.473 Å in orschallite, Weidenthaler et al. 1993). Ca2-O distances are in the range 2.317–2.398 Å (Table 3), with a mean value (2.358 Å) similar to that observed for the octahedral <Ca-OH> distance in the crystal structure of portlandite (2.371 Å, Busing and Levy 1957).

The B layer is characterized by a high degree of structural disorder; no electron density peaks, however, were located away from a narrow sheet at *y* = 0, ½ (maximum shift from the plane was observed for Ow2 at *y* = 0.473). Therefore, it was not possible to identify any thiosulfate groups. Taking into account the spectroscopic results, we interpreted the peaks in the B layer as a disordered assemblage of planar $S_n^{2-}$ groups. Indeed, due to the rather low occupancy of most S positions (Table 1), the simultaneous presence of selected S atoms with unreliable S-S separations can be reasonably disregarded. Instead, groups of three, or, to a lesser extent, four S atoms having suitable distances (2.00–2.24 Å) and angles (100–104°) for $S_3^{2-}$ and $S_4^{2-}$ polyanions can be recognized (Table 3). These values match the S-S distances and S-Ŝ-S angles commonly observed in planar polysulfide groups (2.0595 Å and 110.6°, Cox and Wardell 1997; 2.052–2.060 Å and 107.0°, Gallacher and Pinkerton 1992; 2.016–2.136 Å and 103.8°, Freeman et al. 1995; 2.048 Å and 104.0, Stoll and Bensch 2003). Taking into account the low occupancy of each sulfur atom, it can be assumed that $S_3^{2-}$ [i.e., S5-S1-S4(v), S4(v)-S1-S4(vi), S4(v)-S2-S6(v), S6-S2(v)-S4, S2(v)-S4-S1(iv)] or $S_4^{2-}$ [i.e., S6-S2(v)-S4-S1(iv)] groups have a different probability of occurring in the B layer. The sulfur

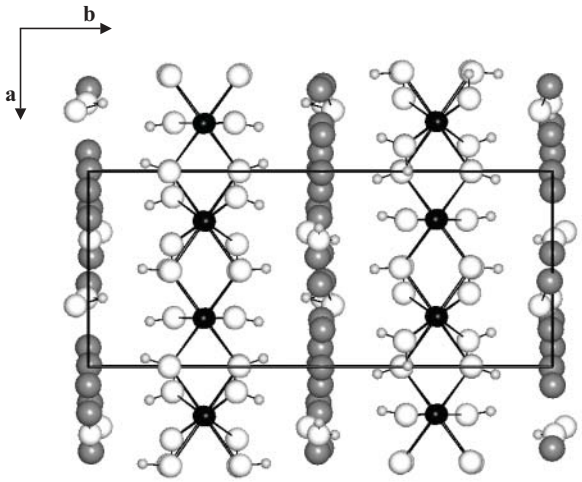


**FIGURE 2.** The crystal structure projected down [001]. Black, dark gray, light gray, and white circles refer to Ca, S, hydrogen, and O atoms, respectively. The unit cell is outlined.

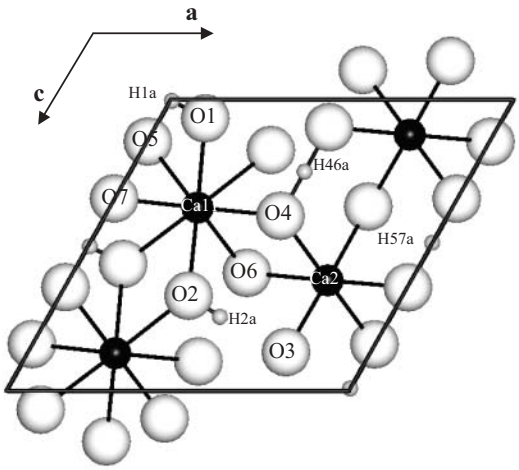


**FIGURE 3.** The A-layer projected down [010]. The symbols are as in Figure 3. The unit cell is outlined.

atoms mostly involved in possible $S_3$ fragments are S1, S2, and S4 in keeping with their higher occupancy factor. On the contrary, the S3 atom (s.o.f. = 0.34) is consistent only with the S3-S1-S4(vi) fragment, which, however, does not fit the geometrical requirements of the $S_3^{2-}$ group as closely as the other fragments (Table 3). Keeping in mind the spectroscopic results showing that S is likely present in the condensed $H_2S$ form as well, one can speculate that, if present, such a molecule is located at the S3 position. However, associated hydrogen atoms were not located on the $\Delta F$-Fourier map.

## HYDROGEN-BONDING MODEL

Every oxygen atom in the A layer links only two Ca ions and only hydrogen atoms occur between the layer of Ca polyhedra (layer A) and the sheet of sulfur atoms at $y = 0, ½$ (layer B). Therefore, it was reasonably hypothesized, in accordance with the spectroscopic results, that both Ca1 and Ca2 atoms are coordinated by $OH^-$ or $H_2O$ groups, and that some of the hydrogen atoms must point toward the B layer, which allows the connection between the oxygen atoms belonging to the A layer and the negatively charged B layer. On the $\Delta F$-Fourier map, only a few hydrogen atoms were unambiguously located (see Table 1). Nevertheless, the positions of some of these (namely H1b, H3b, H4b, and H5b) have $y \sim 0.36$, thus supporting the above assumption. On the other hand, H1a, H2a, H46a, and H57a are located at $y \sim 0.32$, that is, within the sheet of the oxygen atoms. Bond-valence sums for all oxygen atoms belonging to the A layer were calculated according to the bond-valence method of Brown and Altermatt (1985) and taking into account only the Ca-O bonds (Table 4). Bond-valence sums for both O1 and O2 (0.42 v.u.), which link two eight-coordinated Ca1 ions, support the hypothesis that not only O1 (which links H1a and H1b) but also O2 (only H2a as experimental evidence) belong to water molecules. Because of the presence of hydrogen atoms located approximately on the same sheet of O atoms ($y \sim 0.32$), the O···O distances suitable for hydrogen bonds were examined. There are only four independent O···O contacts within the A layer which are not polyhedral edges. These are the following: $d$[O1···O3(iv)] = 2.78(1) Å, $d$[O2···O3] = 2.76(1) Å, $d$[O4···O6(ii)]

**TABLE 3.** Selected bond distances (Å) and angles (°) for the crystal examined

| | | | | | | | |
|---|---|---|---|---|---|---|---|
| Ca1 | - O5 | 2.395(9) | Ca2 | - | O7(iii) | | 2.317(7) |
| | O6 | 2.397(9) | | | O3(ii) | | 2.341(9) |
| | O4 | 2.427(9) | | | O3 | | 2.353(8) |
| | O7 | 2.45(1) | | | O4 | | 2.361(9) |
| | O2 | 2.52(1) | | | O6 | | 2.376(8) |
| | O1 | 2.53(1) | | | O5(iii) | | 2.398(8) |
| | O1(i) | 2.56(1) | | | | | |
| | O2(ii) | 2.58(1) | | | mean | | 2.358 |
| | mean | 2.482 | | | | | |
| O5 | - Ca1 - O6 | 115.0(3) | O7(iii) | - | Ca2 - O3(ii) | | 93.6(3) |
| | - Ca1 - O4 | 140.1(3) | | - | Ca2 - O3 | | 88.7(3) |
| | - Ca1 - O7 | 78.7(3) | | - | Ca2 - O4 | | 179.1(2) |
| | - Ca1 - O2 | 143.7(3) | | - | Ca2 - O6 | | 99.6(3) |
| | - Ca1 - O1 | 72.9(3) | | - | Ca2 - O5(iii) | | 81.4(2) |
| | - Ca1 - O1(i) | 76.6(3) | O3(ii) | - | Ca2 - O3 | | 177.5(2) |
| | - Ca1 - O2 | 74.8(3) | | - | Ca2 - O4 | | 86.8(3) |
| O6 | - Ca1 - O4 | 79.5(3) | | - | Ca2 - O6 | | 92.2(3) |
| | - Ca1 - O7 | 141.2(3) | | - | Ca2 - O5(iii) | | 88.1(2) |
| | - Ca1 - O2 | 75.1(3) | | - | Ca2 - O4 | | 91.0(3) |
| | - Ca1 - O1 | 144.1(3) | | - | Ca2 - O6 | | 88.5(3) |
| | - Ca1 - O1(i) | 75.7(3) | | - | Ca2 - O5(iii) | | 91.2(3) |
| | - Ca1 - O2(ii) | 76.4(3) | O4 | - | Ca2 - O6 | | 81.2(2) |
| O4 | - Ca1 - O7 | 114.2(3) | | - | Ca2 - O5(iii) | | 97.8(3) |
| | - Ca1 - O2 | 74.4(3) | O6 | - | Ca2 - O5(iii) | | 178.9(2) |
| | - Ca1 - O1 | 75.2(3) | | | | | |
| | - Ca1 - O1(i) | 142.5(3) | S1 | - | S3 | | 2.33(3) |
| | - Ca1 - O2(ii) | 73.1(3) | | - | S4(vi) | | 2.19(2) |
| O7 | - Ca1 - O2 | 74.4(3) | S3 | - | S1 - S4(vi) | | 125(1) |
| | - Ca1 - O1 | 73.5(3) | | | | | |
| | - Ca1 - O1(i) | 72.7(3) | S1 | - | S4(v) | | 2.14(3) |
| | - Ca1 - O2(ii) | 141.4(3) | | - | S5 | | 2.00(3) |
| O2 | - Ca1 - O1 | 120.6(3) | S5 | - | S1 - S4(v) | | 100(1) |
| | - Ca1 - O1(i) | 72.5(3) | | | | | |
| | - Ca1 - O2(ii) | 140.0(3) | S1 | - | S4(v) | | 2.14(3) |
| O1 | - Ca1 - O1(i) | 138.0(3) | | - | S4(vi) | | 2.19(2) |
| | - Ca1 - O2(ii) | 72.2(3) | S4(v) | - | S1 - S4(vi) | | 100(1) |
| O1(i) | - Ca1 - O2(ii) | 126.0(3) | | | | | |
| | | | S2 | - | S4(v) | | 2.00(3) |
| | | | | - | S6(v) | | 2.24(2) |
| | | | S4(v) | - | S2 - S6(v) | | 104(1) |
| O1 | - O3(iv) | 2.78(1) | | | | | |
| O2 | - O3 | 2.76(1) | S4 | - | S1(iv) | | 2.19(2) |
| O4 | - O6(ii) | 2.48(1) | | - | S2(v) | | 2.00(3) |
| O5 | - O7(ii) | 2.49(1) | S1(iv) | - | S4 - S2(v) | | 102(1) |

*Note:* Symmetry codes are: (i): $x, ½ - y, ½ + z$; (ii): $x, ½ - y, -½ + z$; (iii): $1 + x, ½ - y, ½ + z$; (iv): $-1 + x, y, -1 + z$; (v): $-x + 1, -y + 1, -z + 1$; (vi):$1 + x, y, 1 + z$.

**TABLE 4.** Bond-valence (v.u.) arrangement for the crystal examined

| | O1 | O2 | O3 | O4 | O5 | O6 | O7 | |
|---|---|---|---|---|---|---|---|---|
| Ca1 | 0.221 | 0.224 | | 0.288 | 0.315 | 0.313 | 0.269 | 2.023 |
| | 0.200 | 0.193 | | | | | | |
| Ca2 | | | 0.364 | 0.345 | 0.312 | 0.331 | 0.388 | 2.092 |
| | | | 0.352 | | | | | |
| * | 0.421 | 0.417 | 0.716 | 0.633 | 0.627 | 0.644 | 0.657 | |
| H1a | 0.75 | | 0.25 | | | | | |
| H2a | | 0.75 | 0.25 | | | | | |
| H46a | | | | 0.50 | | 0.50 | | |
| H57a | | | | | 0.50 | | 0.50 | |
| Hb(1-7) | 0.85 | 0.85 | 0.85 | 0.85 | 0.85 | 0.85 | 0.85 | |
| | 2.02 | 2.02 | 2.07 | 1.98 | 1.98 | 1.99 | 2.01 | |

*Note*: Calculated from the bond-valence curves of Brown and Altermatt (1985).
* Bond-valence sums calculated without contributions of hydrogen atoms

= 2.48(1) Å, and *d*[O5···O7(ii)] = 2.49(1) Å. Taking into account the deduction that both O1 and O2 belong to water molecules, it can be supposed that O3 (which links H3b out of the layer) acts as an acceptor of hydrogen bonds from both O1 and O2. Thus, the following hydrogen-bonding model was assumed: O2 → O3 and O1 → O3. For the other two O···O contacts two hydrogen bonding schemes are possible, O4 ↔ O6 and O5 ↔ O7, with both O4 or O6, and O5 or O7 suitable donor oxygen atoms. Indeed, the position of the hydrogen atoms located on the Δ*F*-Fourier map is consistent with symmetrical hydrogen bonds for both O4···O6 and O5···O7 bridges. This is in keeping with the calculated bond-valence sums (0.63, 0.63, 0.64, and 0.66 v.u. for O4, O5, O6, and O7, respectively) and also with the observed donor-acceptor distances (2.483 and 2.486 Å), which are shorter than those observed for asymmetrical hydrogen bonds. Indeed, it is well known that as the O···O distance decreases to about 2.5 Å, the hydrogen bond becomes symmetrical (Hamilton and Ibers 1968). Of course, it is not easy to solve definitively from X-ray diffraction data whether or not the hydrogen atoms are really centered between the oxygen positions or if a disordered mode of hydrogen bonding occurs. In serandite (Jacobsen et al. 2000) a hydrogen atom statistically occupies two slightly asymmetrical positions along a very short O···O contact [*d*(O···O) = 2.464(1) or 2.467(1) Å from X-ray or neutron diffraction data, respectively].

Considering the proposed hydrogen-bonding system, oxygen bond-valence sums were recalculated by adding contributions of the hydrogen atoms as follows: 0.75 and 0.25 v.u. were assigned to donor and acceptor O atoms, respectively, whereas a bond strength of 0.5 v.u. was added to each oxygen atom involved in the symmetrical hydrogen bonds. Taking into account the weak interactions between Hb atoms and the polysulfide sheet ($O_{A\text{-layer}}$ ···$S_{B\text{-layer}}$ interdistances longer than 3.11 Å), a bond strength of 0.85 v.u. was tentatively assigned to the interlayer O-Hb bonds. The contribution of the interlayer Hb atoms was also assigned to O2, O6, and O7, although no Hb atom was located on the Δ*F*-Fourier map. The final bond strengths (Table 4) support the hypothesized hydrogen-bonding system. Due to uncertainty in determining the actual chemical species located at the partially occupied Ow1 and Ow2 positions (only tentatively assigned to water molecules), the contribution of associated hydrogen bonding was not taken into account.

## TWINNING

The coexistence of two crystal domains related by a (100) twin plane (monoclinic orientation) means that the nodes of the reciprocal lattice of the first individual component perfectly overlap with the nodes of the other individual (Miller indices of the superimposed reflections are $h_I\, k_I\, l_I$ for the first domain, and $h_{II} = -h_I - l_I$, $k_{II} = k_I$, $l_{II} = l_I$ for the second domain). Thus, the ratio of the nodes in the twin cell and in the individual cell is 1. Therefore, twinning in bazhenovite can be classified as *merohedric*, with the twin index $n_T = 1$. According to Nespolo and Ferraris (2003), indeed, the adjective *merohedric* or *non-merohedric* should be preferred to the more ambiguous *merohedral* or *non-merohedral* to avoid any confusion with the characteristics of the individual, which may exhibit a merohedral or non-merohedral point symmetry. According to the criteria of the new classification recently proposed by Nespolo and Ferraris (2004), this case [$n_T = 1$; D(L) ⊃ D(H)] corresponds to twinning by *metric merohedry*.

## CONCLUDING REMARKS

On the basis of the hydrogen-bonding model, the chemical formula $\{[Ca_2(H_2O)_4(OH)_3]_2\}^{2+}$ was assigned to the A layer. The sum of the site occupancy factors for the S atoms in a B layer yields 2 × 2.19 = 4.38. By supposing arbitrarily that all S atoms are only bound in $S_3^{2-}$ groups, a negatively charged B layer $[(H_2O)(S_3^{2-})_{1.46}]^{2.92-}$ would result. Even assuming the presence of a few $S_4^{2-}$ and $S_5^{2-}$ groups, neutrality is hardly achieved. The possibility that S is present in the condensed form $H_2S$ as well, as revealed by Raman investigation, could play a crucial role in decreasing the negative charge of the B layer.

Both structural and spectroscopic data support the conclusion that the mineral examined does not contain thiosulfate groups. However, the question arises as to whether or not the mineral can still be considered as unaltered or has lost components since its discovery. Table 5 compares the X-ray observed powder patterns of the examined mineral (2), the original bazhenovite (3), and synthetic $CaS_5{\cdot}CaS_2O_3{\cdot}6Ca(OH)_2\cdot 20H_2O$ compound (4) with that calculated on the basis of the structural model proposed here (1). The observed *d*-spacing values give unit-cell dimensions similar enough to exclude extensive variations in composition. Nonetheless, the unit-cell volume decreases slightly on going from the synthetic compound (2137.2 / 2 = 1068.6 Å$^3$) to the original bazhenovite (1059 Å$^3$) to the mineral examined in this study [1043.2(8) or 1044.2(6) Å$^3$ from single-crystal or powder diffraction data, respectively]. The decrease is anisotropic, mainly affecting the *b* parameter: 17.65 Å for the synthetic compound, 17.47(1) Å for the original bazhenovite sample, and 17.346(6) Å [or 17.349(6) Å] for the sample examined in this study. Such a decrease could indeed correspond to some changes in the B layer, namely the loss of the thiosulfate group. Furthermore, the relative intensities of the observed powder patterns (Table 5) show pronounced differences. In particular, the observed powder pattern obtained for the sample studied here closely matches that calculated on the basis of the proposed structural model, while the original bazhenovite exhibits strong reflections which are only weak or very weak in our sample. Even stronger and more numerous peaks are present in the diffraction pattern of the synthetic compound, which exhibits an IR spectrum supporting the presence of the thiosulfate group (Lutz et al. 1969). A complete spectroscopic characterization is not given in the original description of the mineral, wherein the only spectral feature possibly due to the $S_2O_3^{2-}$ group is that at 1100 cm$^{-1}$ (Chesnokov et al. 1987),

which was not observed in our sample.

According to Witzke and Göske (2002), the unusual assemblage containing bazhenovite at the Ronneburg mining area represents a non-equilibrium association, as shown by the several sulfur valencies in the associated minerals: $S^{2-}$ (oldhamite), $S^0$ (native sulfur), $S^{4+}$ (sulfite in hannebachite), and $S^{6+}$ (sulfate in gypsum, anhydrite, and ettringite). Bazhenovite at the type locality is associated with oldhamite and native sulfur. Therefore, the genesis of bazhenovite can represent an intermediate stage of sulfur oxidation from sulfide to sulfate, along a stepwise sequence including sulfides, trisulfides, elemental sulfur, thiosulfates, up to sulfites and sulfates. Braithwaite et al. (1993) identified natural intermediate phases in the oxidative weathering of BaS to $BaSO_4$, including two barium thiosulfates, a barium sulfite, and a hydrated barium aluminium hydroxy-trisulfide. The latter compound is described as a monoclinic $P2_1/c$ layer-lattice hydroxide interlayered with trisulfide ions and water molecules. A complete structural characterization, however, was not reported by Braithwaite et al. (1993). By analogy with the process described by these authors for the gradual oxidation of BaS (found at a smelting mill in mineralizations wherein baryte was an important gangue mineral), it can be hypothesized that different intermediate phases can be formed during the alteration path of oldhamite toward Ca-bearing sulfates. Bazhenovite and the mineral here examined, therefore, could represent two distinct phases slightly differing from each other with respect to the thiosulfate content.

**TABLE 5.** X-ray powder diffraction patterns for bazhenovite-like phases

| | 1 | | 2 | | 3 | | 4 | |
|---|---|---|---|---|---|---|---|---|
| *hkl* | $d_{calc}$ (Å) | $I/I_o$ | $d_{obs}$ (Å) | $I/I_o$ | $d_{obs}$ (Å) | $I/I_o$ | $d_{obs}$ (Å) | $I/I_o$ |
| 020 | 8.6730 | 100 | 8.67 | 100 | 8.76 | 100 | 8.83 | 100 |
| $\bar{1}11$ | 6.6238 | 25 | 6.60 | 20 | 6.75 | 10 | 6.70 | 40 |
| $\bar{1}31$ | 4.5001 | 9 | 4.50 | 10 | 4.52 | 20 | – | – |
| 040 | 4.3365 | 74 | 4.32 | 65 | 4.39 | 100 | 4.41 | 100 |
| $\bar{1}02$ | 4.1105 | 9 | 4.11 | 5 | 4.16 | 10 | 4.12 | 20 |
| – | – | – | – | – | – | – | 3.86 | 20 |
| $\bar{1}22$ | 3.7144 | 13 | 3.71 | 20 | 3.75 | 20 | 3.74 | 20 |
| – | – | – | – | – | – | – | 3.60 | 20 |
| 220 | 3.3702 | 9 | 3.36 | 5 | 3.37 | 10 | 3.39 | 40 |
| 022 | 3.3120 | 5 | 3.31 | 5 | – | – | – | - |
| – | – | – | – | – | – | – | 3.22 | 20 |
| – | – | – | – | – | – | – | 3.13 | 20 |
| $\bar{1}42$ | 2.9833 | 25 | 2.99 | 25 | 3.01 | 30 | 3.02 | 60 |
| 060 | 2.8910 | 18 | 2.89 | 20 | 2.91 | 60 | 2.939 | 60 |
| 240 | 2.7959 | 26 | 2.80 | 30 | 2.81 | 50 | 2.829 | 60 |
| 211 | 2.7226 | 10 | 2.72 | 10 | 2.74 | 10 | 2.752 | 40 |
| 221 | 2.6272 | 4 | 2.64 | 5 | | | | |
| 122 | 2.6063 | 14 | 2.61 | 30 | 2.62 | 50 | 2.623 | 80 |
| $\bar{3}22$ | 2.6062 | 27 | | | | | | |
| $\bar{1}23$ | 2.5723 | 4 | 2.57 | 5 | – | – | – | – |
| $\bar{3}31$ | 2.4884 | 4 | 2.49 | 5 | – | – | 2.500 | 40 |
| $\bar{2}33$ | 2.4416 | 6 | 2.44 | 5 | – | – | – | – |
| $\bar{1}62$ | 2.3647 | 13 | 2.37 | 20 | 2.38 | 40 | 2.390 | 40 |
| 142 | 2.3119 | 6 | 2.31 | 5 | 2.34 | 20 | 2.296 | 60 |
| 260 | 2.2681 | 21 | 2.27 | 20 | 2.28 | 50 | | |
| – | – | – | – | – | – | – | 2.210 | 40 |
| – | – | – | – | – | – | – | 2.108 | 20 |
| – | – | – | – | – | – | – | 2.061 | 20 |
| $\bar{2}51$ | 2.1583 | 7 | 2.16 | 10 | 2.17 | 20 | – | – |
| $\bar{2}24$ | 1.9999 | 4 | 1.998 | 5 | 1.996 | 70 | 2.005 | 60 |
| 162 | 1.9859 | 14 | 1.984 | 30 | – | – | – | – |
| $\bar{3}62$ | 1.9858 | 18 | | | – | – | – | – |
| $\bar{1}82$ | 1.9178 | 10 | 1.918 | 10 | 1.930 | 40 | 1.939 | 40 |
| 280 | 1.8652 | 8 | 1.866 | 10 | 1.873 | 40 | 1.889 | 40 |
| $\bar{2}44$ | 1.8572 | 6 | 1.859 | 5 | – | – | – | – |
| 400 | 1.8288 | 6 | 1.827 | 5 | 1.840 | 10 | 1.838 | 40 |
| 004 | 1.7918 | 6 | 1.793 | 10 | 1.798 | 40 | 1.799 | 60 |
| 420 | 1.7895 | 5 | | | | | | |
| 024 | 1.7547 | 6 | 1.755 | 15 | – | – | 1.752 | 60 |
| $\bar{4}24$ | 1.7547 | 8 | | | – | – | | |
| – | – | – | – | – | 1.709 | 20 | 1.724 | 20 |
| – | – | – | – | – | 1.680 | 20 | 1.674 | 40 |
| 322 | 1.6408 | 4 | 1.642 | 5 | 1.646 | 30 | 1.646 | 20 |
| – | – | – | – | – | 1.601 | 20 | – | – |
| – | – | – | – | – | 1.570 | 10 | 1.563 | 20 |
| $\bar{3}.10.2$ | 1.4644 | 4 | 1.466 | 5 | 1.470 | 30 | 1.483 | 20 |
| 0.12.0 | 1.4455 | 5 | 1.445 | 5 | 1.452 | 30 | 1.467 | 20 |
| – | – | – | – | – | 1.371 | 20 | – | – |

*Notes:* 1 = powder pattern and indexing calculated on the basis of $a = 8.391(2)$, $b = 17.346(6)$, and $c = 8.221(4)$ Å, $\beta = 119.33(5)°$ and atomic coordinates reported in Table 1 using XPOW software version 2.0 (Downs et al. 1993). Only reflections with $I \geq 4\sigma(I)$ are listed; 2 = observed powder pattern for the bazhenovite sample studied here [114.6 mm Gandolfi camera (Ni-filtered Cu$K\alpha$)]; 3 = observed powder pattern originally reported by Chesnokov et al. (1987); 4 = observed powder pattern reported by Lutz et al. (1969) for the synthetic $CaS_5 \cdot CaS_2O_3 \cdot 6Ca(OH)_2 \cdot 20H_2O$ compound.

## ACKNOWLEDGMENTS

The authors thank B.V. Chesnokov for providing the bazhenovite sample and M. Mauro (University of Florence) for assistance with FTIR measurements. This work was funded by C.N.R. (Istituto di Geoscienze e Georisorse, sezione di Firenze) and by M.I.U.R., CoFin2003, project "Structural complexity in minerals: modulation and modularity."

## REFERENCES CITED

Braithwaite, R.S.W., Kampf, A.R., Pritchard, R.G., and Lamb, R.P.H. (1993) The occurrence of thiosulfates and other unstable sulfur species as natural weathering products of old smelting slags. Mineralogy and Petrology, 47, 255–261.

Brown, I.D. and Altermatt, D. (1985) Bond-valence parameters obtained from a systematic analysis of the inorganic crystal structure database. Acta Crystallographica, B41, 244–247.

Busing, W.R. and Levy, H.A. (1957) Neutron diffraction study of calcium hydroxide. Journal of Chemistry and Physics, 26, 563–568.

Chesnokov, B.V., Polyakov, V.O., and Bushmakin, A.F. (1987) Bazhenovite $CaS_5 \cdot CaS_2O_3 \cdot 6Ca(OH)_2 \cdot 20H_2O$—A new mineral. Zapiski Vsesoiusnogo Mineralnogo Obshchestva, 116, 737–743.

Chivers, T. and Lau, C. (1982) Raman spectroscopic identification of the $S_4N^-$ and $S^{3-}$ ions in blue solutions of sulphur in liquid ammonia. Inorganic Chemistry, 21, 453–455.

Cox, P.J. and Wardell, J.L. (1997) A polymorph of bis(2-nitrophenyl) trisulfide. Acta Crystallographica, C53, 122–124.

Degen, I.A. and Newman, G.A. (1993) Raman spectra of inorganic ions. Spectrochimica Acta, 49, 859–887.

Downs, R.T., Bartelmehs, K.L., Gibbs, G.V., and Boisen, M.B. Jr. (1993) Interactive software for calculating and displaying X-ray or neutron powder diffractometer patterns of crystalline materials. American Mineralogist, 78, 1104–1107.

Freeman, F., Ma, X.B., and Ziller, J.W. (1995) Bis(tert-butylsulfonyl) disulfide. Acta Crystallographica, C51, 661–663.

Gallacher, A.C. and Pinkerton, A.A. (1992) bis(diethylthiophosphoryl) trisulfide. Acta Crystallographica, C48, 701–703.

Hamilton, W.C. and Ibers, J.A. (1968) Hydrogen bonding in solids: Methods of molecular structure determination, p. 284. Benjamin, New York.

Herzberg, G. (1945) Infrared and Raman Spectra of Polyatomic Molecules, p. 283. Molecular Spectra and Molecular Structure, vol. 2. Nostrand, New York.

Ibers, J.A. and Hamilton, W.C. Eds. (1974) International Tables for X-ray Crystallography, vol. IV, 366p. Kynock, Dordrecht, The Netherlands.

Jacobsen, S.D., Smyth, J.R., Swope, R.J., and Sheldon, R.I. (2000) Two proton positions in the very strong hydrogen bond of serandite, $NaMn_2[Si_3O_8(OH)]$. American Mineralogist, 85, 745–752.

Janz, G.J., Coutts, J.W., Downey, J.R., and Roduner, E. (1976a) Raman studies of sulphur-containing anions in inorganic polysulphides. Potassium polysulphides. Inorganic Chemistry, 15, 1755–1758.

Janz, G.J., Downey, J.R., Roduner, E., Wasilczyk, G.J., Coutts, J.W., and Eluard, A. (1976b) Raman studies of sulphur-containing anions in inorganic polysulfides. Sodium polysulfides. Inorganic Chemistry, 15, 1759–1763.

Janz, G.J., Roduner, E., Coutts, J.W., and Downey, J.R. (1976c) Raman studies of sulphur-containing anions in inorganic polysulfides. Barium trisulfide. Inorganic Chemistry, 15, 1751–1754.

Lutz, Von H.D., Kostic, L.J., and Lochmann, D.D. (1969) Zur Kenntnis der Calciumpolysulfide. Roentgenographische und IR-spektroskopische Untersuchungen an Buchners Kristallen. Zeitschrift für Anorganische und Allgemeine Chemie, 365, 288–293.

Moore, A.E. and Taylor, H.F.W. (1970) Crystal structure of ettringite. Acta Crystallographica, B26, 386–393.

Nespolo, M. and Ferraris, G. (2003) Geminography—The science of twinning applied to the early-stage derivation of non-merohedric twin laws. Zeitschrift für Kristallographie, 218, 178–181.

——— (2004) Applied geminography—Symmetry analysis of twinned crystals and definition of twinning by reticular polyholohedry. Acta Crystallographica, A60, 89–95.

North, A.C.T., Phillips, D.C., and Mathews, F.S. (1968) A semiempirical method of absorption correction. Acta Crystallographica, A24, 351–359.

Pratt, C.S., Coyle, B.A., and Ibers, J.A. (1971) Redetermination of the structure nitrosylpenta-amminecobalt (III) dichloride. Journal of Chemical Society A, 2146–2151.

Ross, S.D. (1972) Inorganic infrared and Raman spectra. McGraw-Hill, New York.

Ryskin, Ya. I. (1974) The Vibrations of Protons in Minerals: Hydroxyl, Water and Ammonium. In V. C. Farmer Ed., The Infrared Spectra of Minerals, Mineralogical Society Monograph 4, Mineralogical Society Publisher, London, pp. 137–182.

Sheldrick, G.M. (1997a) SHELXS-97. A program for automatic solution of crystal structures. University of Göttingen, Germany.

——— (1997b) SHELXL-97. A program for crystal structure refinement. University of Göttingen, Germany.

Stoll, P. and Bensch, W. (2003) $Rb_6Nb_4S_{24.4}O_{0.6}$. Acta Crystallographica, E59, i4-i6.

Weidenthaler, C., Tillmanns, E., and Hentschel, G. (1993) Orschallite, $Ca_3(SO_3)_2SO_4.12H_2O$, a new calcium-sulfite-sulfate-hydrate mineral. Mineralogy and Petrology, 48, 167–177.

Witzke, T. and Göske, J. (2002) An unusual association containing oldhamite, bazhenovite, ye'elimite, hannebachite and other minerals from Ronneburg, Thuringia, Germany. IMA Congress, Edinburgh 2002, Program with abstracts, A77.

MANUSCRIPT RECEIVED AUGUST 3, 2004
MANUSCRIPT ACCEPTED FEBRUARY 11, 2005
MANUSCRIPT HANDLED BY PETER BURNS